NeuroImage: Clinical 19 (2018) 948–962

Contents lists available at ScienceDirect

NeuroImage: Clinical

journal homepage: www.elsevier.com/locate/ynicl

Test-retest variability of resting-state networks in healthy aging and prodromal Alzheimer's disease

Conwell K.[a,c,1], von Reutern B.[a,b,1], Richter N.[a,b], Kukolja J.[a,b], Fink G.R.[a,b], Onur O.A.[a,b,*]

[a] Department of Neurology, University Hospital of Cologne, Cologne 50937, Germany
[b] Cognitive Neuroscience, Institute of Neuroscience and Medicine (INM-3), Research Centre, Jülich 52428, Germany
[c] Department of General, Abdominal, Endocrine and Minimally Invasive Surgery, Academic Hospital Bogenhausen, 81925 Munich, Germany

ARTICLE INFO

Keywords:
ICA
MCI
fMRI
DMN

ABSTRACT

In recent years, changes in resting-state networks (RSN), identified by functional magnetic resonance imaging (fMRI), have gained increasing attention as potential biomarkers and trackers of neurological disorders such as Alzheimer's disease (AD). Intersession reliability of RSN is fundamental to this approach.

In this study, we investigated the test-retest reliability of three memory related RSN (i.e., the default mode, salience, and executive control network) in 15 young, 15 healthy seniors (HS), and 15 subjects affected by mild cognitive impairment (MCI) with positive biomarkers suggestive of incipient AD (6 females each). FMRI was conducted on three separate occasions. Independent Component Analysis decomposed the resting-state data into RSNs. Comparisons of variation in functional connectivity between groups were made applying different thresholds in an explorative approach. Intersession test-retest reliability was evaluated by intraclass correlation coefficient (ICC) comparisons. To assess the effect of gray matter volume loss, motion, cerebrospinal fluid based biomarkers and the time gap between sessions on intersession variation, the former four were correlated separately with the latter.

Data showed that i) young subjects ICCs (relative to HS/MCI-subjects) had higher intersession reliability, ii) stringent statistical thresholds need to be applied to prevent false-positives, iii) both HS and MCI-subjects (relative to young) showed significantly more clusters of intersession variation in all three RSN, iv) while intersession variation was highly correlated with head motion, it was also correlated with biomarkers (especially phospho-tau), the time gap between sessions and local GMV. Results indicate that time gaps between sessions should be kept constant and that head motion must be taken into account when using RSN to assess aging and neurodegeneration. In patients with prodromal AD, re-test reliability may be increased by accouting for overall disease burden by including biomarkers of neuronal injury (especially phospho-tau) in statistical analyses. Local atrophy however, does not seem to play a major role in regards to reliability, but should be used as covariate depending on the research question.

1. Introduction

Mild cognitive impairment (MCI) is a disorder along the spectrum of normal aging and Alzheimer's disease (AD) (Petersen et al., 1999). The diagnostic entity MCI encompasses a heterogeneous group of patients ranging from subjects with mild depression to prodromal AD. All MCI subjects, but particularly those with a positive biomarker-status, have an increased probability of developing AD (Petersen et al., 2001; Grundman et al., 2004; Mitchell and Shiri-Feshki, 2009). With drug development efforts shifting from the treatment of symptomatic AD to therapeutic interventions at preclinical stages (Vellas et al., 2011; Salomone et al., 2012), early detection of individuals at risk of AD has become increasingly important.

Efforts to use resting-state (RS) functional Magnetic Resonance Imaging (fMRI) for these purposes are in progress, as RS-fMRI is a radiation-free, non-invasive method that does not require active participation of the subject. RS-fMRI reveals functionally connected but anatomically distant brain regions (Barkhof et al., 2014). These regions have consistently been classified into resting-state networks (RSN) as they represent reproducible, large-scale functional brain systems. RSN include but are not limited to the default mode network (DMN), attention network, executive control network (ECN), visual network,

* Corresponding author at: Department of Neurology, University Hospital of Cologne, Kerpener Str. 62, 50937 Köln, Germany.
E-mail address: oezguer.onur@uk-koeln.de (O.A. Onur).
[1] Authors contributed equally.

https://doi.org/10.1016/j.nicl.2018.06.016
Received 20 March 2018; Received in revised form 11 June 2018; Accepted 13 June 2018
Available online 18 June 2018

motor network, auditory-phonological network, and the salience network (SN) (Biswal et al., 1995; Hampson et al., 2002; Fox et al., 2005; Yeo et al., 2011; Buckner et al., 2013). Alterations in these RSN are thought to precede symptoms and structural changes in neurodegeneration by several years, and might allow the identification and quantification of preclinical disease stages (Jack Jr. et al., 2010; Sperling, 2011; Gomez-Ramirez and Wu, 2014).

Since functional connectivity within the DMN of MCI patients shows alterations that differ from general aging-related effects, DMN functional connectivity has become a focus of studies investigating AD-related changes (Sorg et al., 2007; Agosta et al., 2012; Cha et al., 2013). Notably, the DMN comprises the hippocampus and the precuneus, regions well-known to be involved in early stages of AD. However, the scope of RSN studies extends beyond the DMN and it has been suggested that two RSN may prove particularly suitable for assessing early AD-related changes: the salience network and the executive control network (Seeley et al., 2007, Menon and Uddin, 2010).

A reproducible and reliable baseline is a mandatory prerequisite for the use of RSN as biomarkers (Zhang et al., 2010) and trackers of treatment effects (Goekoop et al., 2004; Dickerson and Sperling, 2005). Test-retest (TRT) reliability of RSN might be, at least in part, influenced by various factors, such as physiological confounds, scanning conditions, data analysis strategy, differences in brain anatomy or gray matter volume, head motion, disease progression, cerebralspinal fluid based biomarkers, and so forth. To date, only a few studies have investigated the TRT reliability of RSN (Damoiseaux et al., 2006; Shehzad et al., 2009; Meindl et al., 2010; Zuo et al., 2010; Chou et al., 2012; Guo et al., 2012). These studies either focused on one age group or compared the TRT reliability between healthy seniors and MCI patients over a period of one year (Blautzik et al., 2013).

In this study we investigated the TRT reliability of three memory-related RSN (DMN, ECN, SN) in healthy young subjects, healthy seniors, and subjects with prodromal AD across three scanning sessions, with approximately two weeks in-between each scanning session (median 14 days, standard deviation 28 days) for each participant. We examined voxel-wise intersession variations in cortical activation patterns and specifically assessed whether gray matter volume (GMV) loss, biomarkers in cerebrospinal fluid, the time gap between acquired sessions and motion are associated with session differences observed. We expected to find i) a higher TRT reliability in young subjects relative to HS and MCI, ii) an increase in intersession variations due to gray matter volume loss and motion (Marchitelli et al., 2016) and to a lesser degree due to biomarkers and the time gap between sessions.

2. Materials and methods

2.1. Subjects

Fifteen healthy young subjects (age: 24.4 ± 2.8 years; six females), fifteen healthy seniors (HS; age: 67.3 ± 8.1 years; six females), and fifteen patients with MCI (age: 71.1 ± 6.0 years; six females) participated in the study. Healthy participants were recruited via local advertisement. MCI patients were recruited from the memory clinic of the Department of Neurology at the University Hospital Cologne. Prior to participation, informed written consent was obtained from all participants. The local ethical committee (medical faculty, University of Cologne) had approved the study. All subjects were right-handed according to the Edinburgh Handedness Inventory (Oldfield, 1971) and completed a medical questionnaire to rule out neuropsychiatric diseases, with exception of amnestic deficits in MCI, as well as the intake of CNS-effective medication. To eliminate the possibility of contradictions to MRI scanning, a safety-checklist was completed.

Since MCI is a diagnostic entity that encompasses a heterogeneous group of individuals (Petersen et al., 2001), we decided to only include subjects who are in the stage of prodromal AD according to the IWG-2 criteria and Dubois et al. (2014, 2016), with at least one abnormal biomarker suggestive of AD, i.e., abnormal concentrations of amyloid β42, phospho-tau, total tau, a pathological total tau - amyloid β42 ratio > 0.52 in cerebrospinal fluid (CSF) obtained by lumbar puncture (Duits et al., 2015), or amyloid-plaque deposition assessed with positron emission tomography (PET).

Subjects underwent neuropsychological assessment including the Mini Mental Status Examination (MMSE) (Folstein et al., 1975), the Trail Making Test (TMT) for visual processing speed, executive functioning and task switching (Tombaugh, 2004; Bowie and Harvey, 2006), a test of auditory verbal learning and memory (Verbaler Lern- und Merkfähigkeitstest, VLMT) (Helmstaedter et al., 2001), a test of logical thinking, conception of space and recognition of patterns and irregularities (LPS50 +, Leistungsprüfungssystem für 50- bis 90-jährige, Subtest 7) (Horn, 1983), the Bayer Activity of Daily Living Scale (B-ADL) (Hindmarch et al., 1998), and the Hamilton Depression Rating Scale to measure subjective symptoms of depression (Hamilton, 1960).

2.2. Experimental setup

FMRI measurements were acquired on three separate occasions, with approximately two weeks in-between each scanning session (median 14 days, standard deviation 28 days) for each participant. The minimum interval between two sessions was 3 days. Each participant underwent all three imaging sessions at the same time of day. Participants were instructed to refrain from caffeine consumption before scanning. During each of these measurements, subjects were asked to lay still with their eyes closed, to think of nothing in particular and not to fall asleep. To account for the influence of fatigue and sleep, participants were monitored through a camera system and asked to retrospectively rate the degree of fatigue they had experienced during scanning on a scale from 1 (not tired) to 6 (very tired). Additionally, subjects were asked whether they had fallen asleep at any point throughout the scanning procedure. Only one MCI subject reported to have fallen asleep briefly during one session, and another was unsure whether sleep might have occurred briefly during one session. Since the periods of sleep were brief and had not been detected by the camera-based monitoring, these subjects were not excluded from further analyses.

2.3. Image acquisition

All functional and anatomical imaging was performed using a TRIO 3.0 Tesla whole-body scanner (Siemens, Erlangen, Germany) equipped with a standard head coil for radiofrequency transmission and signal reception. Sequence parameters were: T2*-weighted echoplanar images (EPI) with BOLD contrast, echo time (TE) = 30 ms, repetition time (TR) = 2430 ms, flip angle = 90°, slice thickness 3.0 mm, interslice gap 0.3 mm, field of view (FoV) = 200 mm, matrix size 64 × 64, in-plane resolution = 3.0 mm × 3.0 mm. 40 axial slices per volume, capturing the brain from vertex to cerebellum were acquired sequentially. 155 volumes were acquired and the first 4 functional volumes of the fMRI time series of each session were discarded from analysis to account for T1 saturation effects. As a result, 151 images were subjected to further analysis. Total acquisition time amounted to approximately 6.3 min per session. The slices were positioned at an angle between a line crossing the anterior and posterior commissure (AC-PC line) and a line paralleling the medial tentorium cerebelli. This resulted in a slice orientation previously proposed to reduce susceptibility artifacts in the medial temporal lobe (Deichmann et al., 2003; Weiskopf et al., 2006). For anatomical reference and to control for gray matter density, a high-resolution T1 image was obtained for each subject using a three-dimensional magnetization-prepared, rapid acquisition gradient echo sequence (MP-RAGE). To control for white matter lesions and macroangiopathy, T2-weighted FLAIR and Time of Flight measurements were performed. None of these or any other imaging procedures preceded the RS fMRI scans.

2.4. Data preprocessing

Image preprocessing was performed using Matlab12 (The MathWorks Inc., Natick, MA) and SPM8 (statistical parametric mapping software, Wellcome Department of Imaging Neuroscience, London, UK; http://www.fil.ion.ucl.ac.uk). Images were spatially realigned to the first volume to correct for head movements and normalized to an EPI template volume in standard stereotactic MNI (Montreal Neurological Institute) space. We refrained from correcting for slice-timing as the expected improvements are minimal (Wu et al., 2011). The images were resampled at $2 \times 2 \times 2\,mm^3$ voxel size. Spatial smoothing was implemented to remove high-frequency fluctuations by means of a 8-mm full-width-half-maximum Gaussian kernel to compensate for residual anatomical variations across subjects (Worsley and Friston, 1995).

2.5. Data analysis

2.5.1. Demographic and neuropsychological data analysis

Statistical analyses were performed using IBM SPSS Statistics 23 for Mac OS 10.10.5. Baseline differences in demographics and overall cognitive performance between the two control groups and MCI subjects were compared with an analysis of variance (ANOVA) for independent samples with a significance level of $\alpha = .05$. Group-wise comparisons were performed using unpaired *t*-tests.

2.5.2. Independent component analysis

Resting state fMRI data was segregated into spatially independent but temporally coherent and functionally connected components on the basis of their statistical features using independent component analysis (ICA). In order to glean the most robust and comparable set of independent components (IC), we carried out one spatial group ICA for the entire group of participants by temporally concatenating all individual data sets from each session and group using the GIFT software (http://icatb.sourceforge.net/, version 2.0 e;) (Calhoun et al., 2001; Beckmann et al., 2005). Referred to as temporal concatenation group ICA (TC-GICA), this method extrapolates group-level components, whose functionally relevant components are termed RSN or intrinsic connectivity networks (ICN). The analysis consisted of four consecutive steps: i) data preprocessing using intensity normalization, the time-series having been scaled to a mean of 100 at each voxel, ii) data reduction with principal component analysis (PCA) to decrease the amount of computation, iii) ICA for the concatenated dataset using the Infomax algorithm, and iv) back-reconstruction of the group independent components into the single-subject space using GICA3 (Erhardt et al., 2011). Since a standard algorithm for computing the ideal number of IC has yet to be established (Cole et al., 2010), we allowed ICA to automatically estimate the number of IC (Calhoun et al., 2001).

2.5.3. Selection of IC representing RSN

For the purpose of selecting the IC that best matched the DMN, SN, and ECN, we followed the algorithm suggested by Franco et al. (2009). First, two raters (KC, OAO) independently sorted the IC extracted by ICA into two groups based on visual inspection: (1) functionally relevant components, (2) components based on artifactual noise, e.g., respiration, head motion etc., and subsequently chose the components that best-fit their empirical notion of each RSN. Then, a commonly employed template matching procedure was implemented (Garrity et al., 2007; Franco et al., 2009; Zuo et al., 2010). Spatial templates of the respective networks were developed based on sets of brain regions of intrinsic resting activity previously ascribed to them. Taking into account that previous publications reported different brain areas constituting the DMN, we opted to create two different DMN templates to reflect this variability. Both templates included the anterior cingulate cortex (ACC), frontal superior gyrus, precuneus, and angular gyrus. One template further included the hippocampus and mid-cingulate cortex (Lim et al., 2014), the other the supramarginal gyrus and posterior-cingulate cortex (PCC) (Franco et al., 2009). The SN template comprised the insula and ACC bilaterally (Raichle, 2011), and the ECN template included the dorsomedial prefrontal cortex (dmPFC) and dorsolateral prefrontal cortex (dlPFC) bilaterally (Agosta et al., 2012). After creating the anatomical templates with the WFU PickAtlas toolbox (version 3.0.4; http://fmri.wfubmc.edu/software/PickAtlas, ANSIR Laboratory, WFU School of Medicine, Winston-Salem, NC, USA), we ran a spatial correlation analysis with GIFT against them, in order to obtain the three components from each template that best resembled each individual RSN.

In a following step, a weighting factor of 3 was assigned to the ACC and PCC of the DMN, whereas the other regions remained weighted at 1 (Franco et al., 2009). The DMN templates were then additionally compared before and after weighting with regard to their top three components and the corresponding spatial correlation coefficient. The top three components for all three RSN selected by each template, were subsequently visually controlled by two raters, additionally verifying goodness of fit. In a final step, the IC chosen by templates and raters were compared for consistency.

2.5.4. Gray matter volume

Gray matter volume (GMV) was quantified utilizing an optimized protocol for voxel-based morphometry (VBM) in SPM8 with the VBM8 toolbox (http://dbm.neuro.uni-jena.de/vbm) (Ashburner and Friston, 2000; Good et al., 2001). For comparisons of GMV between groups, a threshold of $p < 0.05$, corrected for Family-wise Error (FWE) at whole-brain-level was chosen.

2.5.5. Motion parameters

Motion parameters were calculated using the FMRIB Software Library (FSL) motion outliers toolbox (http://fsl.fmrib.ox.ac.uk/fsl/fslwiki/FSLMotionOutliers) (Jenkinson et al., 2012). Since several metrics are available, and it is unknown, which is superior, we opted to calculate four different metrics for each group and session individually: i) refrms: root mean square (RMS) intensity differences of volume n to the reference volume, ii) dvars: RMS intensity difference of volume N to volume N + 1, i.e., a measure of BOLD signal intensity change from one brain image in comparison to a previous time point (Smyser et al., 2010; Power et al., 2012), iii) fd: frame displacement, i.e., average of rotation and translation parameter differences using weighted scaling (Power et al., 2012), and iv) fdrms: frame displacement, i.e., average of rotation and translation parameter differences using a matrix RMS formulation. As the variance of the motion parameters were inhomogeneous according to the Levene's test, Kruskal-Wallis H Tests (Kruskal and Wallis, 1952) were performed using IBM SPSS Statistics 23 for Mac OS 10.10.5 to evaluate whether motion parameters differed significantly between groups. This test, often referred to as one-way analysis of variance (ANOVA) on ranks, differs from an ANOVA in several ways. Among other things, the Kruskal-Wallis H Test is much less sensitive to outliers and does not assume normality in data sets. To ascertain which groups specifically differed from one another, additional Kruskal-Wallis H Tests were carried out, each including only two groups.

2.5.6. Test-retest (TRT) reliability

To assess the reliability of functional connections, the voxel-wise time series were used to calculate intraclass correlation coefficients (ICC) within the ICs (inclusive masking utilizing ICA results). ICCs are a common measure of TRT quantification (Shrout and Fleiss, 1979; Muller and Buttner, 1994; Shehzad et al., 2009; Yan et al., 2016). A 15×3 matrix was created for each group separately, representing the z-transformed correlation values for the 15 subjects of each group, and the 3 scans each subject underwent. We calculated the between-subject mean square (MS_b) and within-subject mean square (MS_w) of variance in connectivity at voxel level. ICC values were then computed according

to the following equation, with k representing the number of sessions (Shrout and Fleiss, 1979): $ICC = \frac{(MSb - MSw)}{MSb + (k-1)MSw}$. ICC maps, representing the respective values at voxel level, were created. The ICC values are categorized into 5 intervals: $0 < ICC \leq 0.2$ (poor), $0.2 < ICC \leq 0.4$ (fair), $0.4 < ICC \leq 0.6$ (moderate), $0.6 < ICC \leq 0.8$ (strong), and $0.8 < ICC < 1$ (almost perfect) (Landis and Koch, 1977).

2.5.7. Comparison of variance between groups

Next, a comparison of connectivity variance (group mean square) within the ICs was conducted between groups by performing an ANOVA, utilizing SPM8. In an explorative approach, three levels of height thresholds, ranging from liberal to conservative, were applied (i. uncorrected $p < 0.001$; ii. $p < 0.001$ to form clusters considered significant at cluster level $p < 0.05$ FWE-corrected; iii. FWE-corrected $p < .05$ on a whole-brain-level). Clusters were required to consist of at least 10 voxels each.

2.5.8. Voxel-wise correlation between variance of functional connectivity and atrophy/motion/biomarkers/time gap between sessions

A voxel-wise correlation between variance of functional connectivity within the respective ICs and VBM maps was performed using SPM8 and the Biological Parametric Mapping toolbox 1.5d (http://fmri.wfubmc.edu/software/BPM) to compute correlation values between variance and cortical atrophy. Resulting statistical maps were thresholded at three levels (i. uncorrected $p < 0.001$; ii. $p < 0.001$ to form clusters considered significant at cluster level $p < 0.05$ FWE-corrected; iii. FWE-corrected $p < 0.05$ on whole-brain-level). A similar approach was chosen to analyze correlation values between variance and motion parameters, biomarker values and the time gap between the three sessions, using these parameters instead of VBM maps.

3. Results

3.1. Demographics, neuropsychological testing, and biomarkers

All groups had the same gender distribution and number of participants. Additionally, HS and MCI groups did not differ significantly in mean age or education. Young subjects had more years of education. Significant differences in cognitive performance between HS and MCI were found in all neuropsychological tests with the exception of the Bayer Activity of Daily Living Scale (B-ADL), which was within normal range for both groups. Subjects had, with the exception of MCI in the patient group, no neuropsychological impairment, the Hamilton score was within normal range and the two groups of healthy subjects (young and seniors) did not show any abnormalities in neuropsychological assessment. For further details see Table 1. The biomarkers, reflecting AD-pathology, are presented in Table 2.

3.2. Selection of IC representing RSN

Based on the concatenated data sets of all participants and sessions, ICA generated 31 IC. Both DMN templates selected the same two IC to best represent the DMN (IC4, IC15; Fig. 1; Table 3). After applying a weighting factor of 3 to the ACC and PCC, the magnitude of correlation increased for IC4 (from 0.29 to 0.33), while that of IC15 slightly decreased (from 0.39 to 0.31). However, both IC remained the top choices for both templates. The components chosen by both raters were consistent with those obtained by the template matching procedure. IC4 predominately included the anterior areas of the DMN, encompassing the dorsal and ventrolateral PFC with activation reaching into the right insular cortex, ACC, superior frontal gyrus, inferior and middle temporal gyrus, temporal pole, parahippocampal gyrus, angular gyrus, superior parietal regions, left inferior parietal gyrus (IPG), right supermarginal gyrus, as well as the caudate nucleus. IC15 mainly comprised the posterior parts of the DMN: the bilateral precuneus / posterior cingulate (PCC) and left cuneus, angular gyrus, superior parietal regions as well as the IPG, midcingulate cortex (MCC), middle temporal gyrus, dlPFC and superior frontal gyrus, all in the left hemisphere. IC19 mainly showed the ACC and midcingulate cortex, as well as the right insula/ temporal pole, with additional involvement of the prefrontal cortex, precuneus, left IPG, right supramarginal gyrus, caudate nucleus, and putamen (Fig. 1; Table 3). This pattern of interconnected brain areas coincides with the SN (Seeley et al., 2007,

Table 1
Neuropsychological and demographic data. Demographics and neuropsychological test results of all three groups. Differences in test results were examined for significance using an ANOVA (factor group), post-hoc group comparisons were analyzed by a two-sample *t*-tests.

Variable	young (n = 15)	HS (n = 15)	MCI (N = 15)	ANOVA	
Age (years)	24.4 (2.9)	67.3 (8.4)	71.1 (6.0)	< 0.001	# §
Education (years)	16.6 (2.1)	14.6 (3.8)	12.5 (3.8)	0.007	§
Female (%)	40	40	40		
MMST	–	29.5 (0.6)	25.0 (3.4)	N/A	†
TMT – A (sec.)	23.7 (8.7)	40 (14.3)	77.2 (43.0)	< 0.001	# § †
TMT – B (sec.)	49.7 (13.6)	87.6 (36.1)	206.7 (100.3)	< 0.001	# § †
VLMT (words):					
Learning	60.3 (6.8)	44.3 (10.4)	27.5 (8.0)	< 0.001	# § †
Recall immediate	13.1 (2.6)	11.1 (2.1)	6.5 (2.0)	< 0.001	§ †
Recall after interference	13.3 (1.2)	8.5 (3.1)	2.6 (2.7)	< 0.001	# § †
Recall after delay	13.3 (1.6)	8.5 (3.1)	2.1 (2.9)	< 0.001	# § †
LPS7	24.4 (5.3)	15.9 (6.6)	11.3 (4.0)[2]	< 0.001	# §
B – ADL	–	2.0 (1.0)[3]	2.8 (1.2)[2]	N/A	
Hamilton	0.5 (0.8)	1.2 (1.7)	2.1 (2.1)[1]	0.047	§

MMST = Mini Mental State Test; TMT = Trail Making Test (TMT-A: numbers; TMT-B: numbers and letters; VLMT = Verbaler Lern- und Merkfähigkeitstest; LPS7 = Leistungsprüfungssystem 7 (visual tasking); B– ADL = Bayer Activities of Daily Living Score; Hamilton = Hamilton Rating Scale of Depression; Edinburgh = Edinburgh Handedness Inventory (R = right handed). $p < 0.05$ in *t*-test young vs HS; [§]$p < 0.05$ in t-test young vs MCI; [†]$p < 0.05$ in t-test HS vs MCI.
[1] n = 14.
[2] n = 12.
[3] n = 6.

Table 2
Biomarkers. Biomarkers suggestive of Alzheimer's disease were gleaned for all MCI subjects. Concentrations of amyloid-beta 42, phospho-tau, total-tau, the ratio of total-tau and amyloid-beta 42 in cerebrospinal fluid, and amyloid-plaque depositions assessed with positron emission tomography were evaluated.

Subject	Aß42 (pg/ml)	PTAU (pg/ml)	TAU (pg/ml)	TAU/Aß42	Amyloid-PET
f 01	546	197	1000	1.8315	N/A
f 02	724	55	409	0.5649	N/A
f 03	582	150	1465	2.5172	N/A
f 04	624	94	656	1.0513	N/A
f 05	384	85	587	1.5286	N/A
f 06	574	98	542	0.9443	N/A
m 01	561	114	1064	1.8966	N/A
m 02	499	61	533	1.0682	N/A
m 03	514	31	189	0.3677	N/A
m 04	402	87	882	2.1940	N/A
m 05	712	110	752	1.0562	N/A
m 06	449	102	842	1.8753	N/A
m 07	618	124	998	1.6149	N/A
m 08	N/A	N/A	N/A	N/A	positive
m 09	N/A	N/A	N/A	N/A	positive

Norms are as follows: amyloid-beta 42 > 650 pg/ml; Phospho-Tau-Protein < 61 pg/ml; Tau-Protein < 400 pg/ml; ratio TAU/Aß42 > 0.52. f = female; m = male; Aß42 = Amyloid-Beta 42; PTAU = Phospho-Tau-Protein; TAU = Tau-Protein.

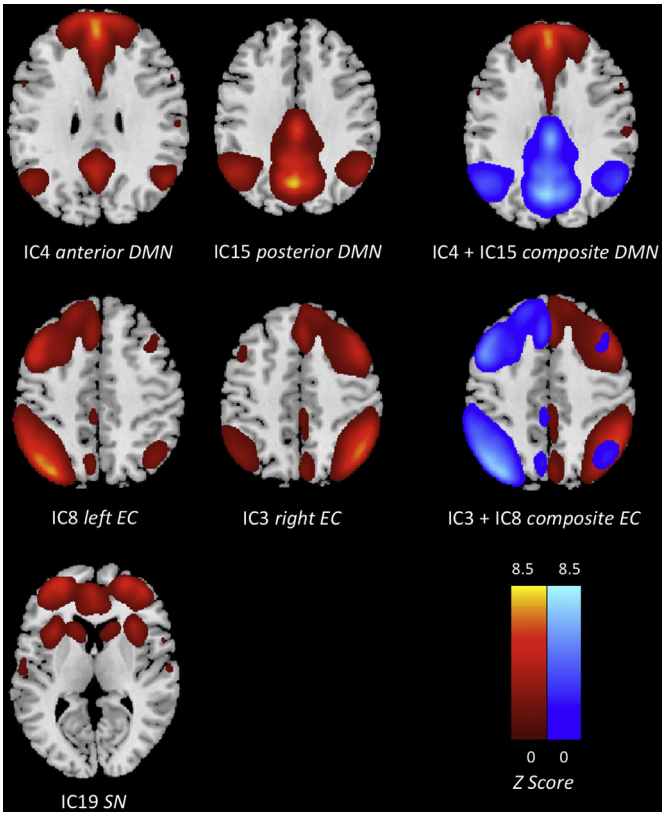

Fig. 1. Independent components best resembling the default mode, executive control, and salience network were obtained via template matching procedure. The DMN and ECN are each represented by two IC, reflecting the anterior and posterior regions of the DMN and the left and right hemisphere of the ECN.

Raichle, 2011, Agosta et al., 2012, Onoda et al., 2012, Lim et al., 2014). IC3 and IC8 represented the right and left side of the ECN, complementing and slightly overlapping each other to form a widespread network including the prefrontal cortex, left ACC, right MCC, inferior and middle temporal gyrus, left insula and lingual gyrus, precuneus/PCC, IPG, angular gyrus, thalamus, as well as parts of the supplementary motor (Fig. 1; Table 3) (Seeley et al., 2007, Zuo et al., 2010, Agosta et al., 2012, Blautzik et al., 2013, Lim et al., 2014). A similar splitting of the DMN and ECN into multiple IC has been observed in previous studies (Damoiseaux et al., 2008; Habas et al., 2009).

3.3. Gray matter volume

Compared with young subjects, HS and MCI showed significant GMV loss in the thalamus and caudate nucleus bilaterally, as well as in the left superior temporal gyrus, with the MCI group exhibiting a higher degree of degeneration in the thalamus bilaterally, right caudate nucleus and the left hippocampus compared to healthy senior controls. MCI showed additional areas of significantly reduced GMV compared to young subjects, including the hippocampus, parahippocampal gyrus, superior temporal gyrus and Heschl's gyrus of the right hemisphere, the insula bilaterally, as well as the lingual gyrus, anterior and mid-cingulate cortex, putamen, and amygdala of the left hemisphere (Fig. 2; Table 4).

3.4. Motion parameters

Compared in a model with the Kruskal-Wallis H Test, the three groups showed significant differences in motion parameters (see Fig. 3). Applying individual comparisons between groups, increased motion was detected for both HS and MCI in contrast to young participants in

Table 3
MNI coordinates of regions contributing to each resting state network. MNI coordinates of anatomical regions contributing to each resting state network. The cluster size is represented by *k* with a cluster extent of 10 voxels corrected for FWE\.05.

Region		Coordinate			*t*	*k*
		x	*y*	*z*		
A. Anterior DMN						
dmPFC	L/R	2	56	34	41.21	16,183
dmPFC	R	6	52	44	37.98	
ACC	R	4	48	14	35.5	
ACC	L	−4	46	4	26.05	
SFG	R	22	34	54	27.36	
SFG	L	−12	48	46	25.47	
IPL (angular gyrus)	L	−50	−66	28	15.42	577
MTG	L	−62	−18	−20	14.49	1160
ITG	L	−60	−6	−28	10.93	
vlPFC	L	−26	16	−14	7.73	
Temporal Pole	L	−46	24	−14	7.72	
IPL (angular gyrus)	R	50	−62	34	13.13	411
MTG	R	60	−4	−24	12.24	1027
ITG	R	48	4	−40	10.43	
Cerebellum	R	34	−80	−34	10.74	307
SPR	R	36	−42	58	10.21	804
IPL (supramarginal gyrus)	R	56	−29	44	6.15	
vlPFC	R	38	32	−16	9.92	294
Insula	R	30	18	−18	6.67	
dlPFC	R	56	30	8	9.72	154
dlPFC	L	−54	24	10	8.05	100
Parahippocampal Gyrus	R	22	−10	−22	6.66	93
Parahippocampal Gyrus	L	−22	−14	−24	6.52	62
IPG	L	−50	−28	44		
Caudate	L	−16	18	4	7.10	76
Caudate	R	12	12	12	5.80	63
B. Posterior DMN						
Precuneus	R	8	−66	38	29.77	8136
Precuneus	L	−2	−70	36	29.61	
MCC	L	−4	−44	36	24.50	
PCC	L	−6	−48	28	23.89	
Cuneus	L	2	−68	26	23.61	
IPL (angular gyrus)	L	−44	−64	43	22.32	2354
IPL (angular gyrus)	R	46	−60	40	20.47	1848
MTG	L	−62	−26	−14	7.06	120
dlPFC	L	−34	12	44	6.02	18
Cerebellum	R	44	−60	−46	6.15	19
SFG	L	−22	58	2	6.12	15
IPG	L	−48	−20	38	6.02	61
SPR	L	−38	−24	40	5.96	
C. Salience Network						
ACC	R	6	28	28	28.17	14,289
SFG	R	38	52	18	28.12	
MCC	R	6	26	36	23.36	
Insula	R	34	18	4	16.87	1670
Temporal Pole	R	50	18	−12	13.54	
vlPFC	R	34	26	−6	11.92	
Caudate	R	20	22	8	8.90	
Putamen	R	32	14	−2	7.15	
SFG	R	20	8	64	10.45	319
Precuneus	L/R	2	−40	48	9.23	1205
SFG	L	−20	10	64	8.95	172
dlPFC	L	−22	10	56	6.76	
IPG	L	−56	−46	48	6.67	27
IPL (supramarginal gyrus)	R	56	−40	40	5.92	20
D. Executive control (predominantly right hemispheric)						
IPG	R	48	−56	50	38.63	4817
IPL (angular gyrus)	R	46	−60	42	36.65	
SPR	R	34	−72	52	20.92	
dlPFC	R	34	18	58	27.74	12,686
vmPFC	R	44	52	−2	26.51	
SFG	R	28	62	16	19.61	
dmPFC	R	4	30	46	18.87	
MTG	R	62	−46	−6	20.69	2136
ITG	R	60	−24	−20	15.91	
MCC	R	4	−32	38	18.64	1007

(*continued on next page*)

Table 3 (*continued*)

Region		Coordinate			*t*	*k*
		x	*y*	*z*		
Precuneus	R	6	−70	42	9.48	
Cerebellum	L	−10	−82	−30	16.99	2253
IPL (angular gyrus)	L	−44	−62	52	12.89	934
IPG	L	−52	−50	50	12.35	
vmPFC	L	−46	48	−4	12.89	934
vlPFC	L	−46	42	−14	8.64	
dlPFC	L	−46	20	42	9.30	91
MTG	L	−66	−38	−8	9.06	107
Thalamus	R	8	−26	2	7.04	23
E. Executive control (predominantly left hemispheric)						
IPL (angular gyrus)	L	−44	−68	42	33.63	5267
IPG	L	−48	−48	52	24.52	
Precuneus	L	−8	−72	60	6.98	
dlPFC	L	−44	12	18	31.11	11,295
vlPFC	L	−42	48	0	31.08	
dmPFC	L	−6	32	40	18.76	
ITG	L	−58	−48	−10	23.78	1771
PCC	L	−4	−42	32	17.64	702
Cerebellum	L	38	−70	−42	16.98	1931
vlPFC	R	46	50	−10	12.35	509
dlPFC	R	40	58	6	5.35	
Insula	L	−32	20	0	10.02	116
IPL (angular gyrus)	R	48	−64	46	8.39	192
Thalamus	L	−10	−30	2	7.73	189
Lingual gyrus	L	−8	−36	2	7.53	
ACC	L	−10	38	24	7.55	30
ITG	R	62	−44	−12	6.80	69
MTG	R	66	−42	−4	6.31	
Cerebellum	R	6	−54	−52	6.75	15
SPR	L	−8	−38	74	6.56	54
Gyrus rectus	L	−8	32	−16	5.98	10

Dm/dl/vm/vl PFC = dorsomedial, dorsolateral, ventromedial, ventrolateral prefrontal cortex; ACC/MCC/PCC = anterior/mid/posterior cingulate cortex; SFG = superior frontal gyrus; IPL = inferior parietal lobe; ITG/MTG = inferior/medial temporal gyrus; SPR = superior parietal regions; PG = parahippocampal gyrus; IPG = inferior parietal gyrus; L = left; R = right.

Table 4
Differences in gray matter volume between groups. Differences in gray matter volume between groups were quantified utilizing an optimized protocol for voxel-based morphometry (VBM) with a threshold of $p < 0.05$, corrected for Family-wise Error at whole-brain-level and a cluster extent of 5 voxels. In comparisons to young subjects, HS and MCI showed significant GMV loss

Comparison between groups		Coordinate			*t*	*k*
		x	*y*	*z*		
young > HS						
STG	L	−40	−16	−5	9.28	12
Thalamus	L/R	0	−18	6	8.96	10
Thalamus	L	−2	−19	1	8.63	9
Caudate	R	14	10	6	5.29	6
young > MCI						
Thalamus	L/R	−2	−19	1	14.85	359
STG	L	−42	−16	−5	12.72	70
Caudate	R	9	10	7	12.15	483
Hippocampus	L	−32	−34	−5	12.07	84
Caudate	L	−12	−1	18	11.36	319
Postcentral gyrus	L	−44	−16	34	10.08	15
Hippocampus	R	36	−33	−6	10.07	64
Thalamus	R	6	−12	15	9.84	9
STG	R	45	−7	−9	9.46	47
Heschl's gyrus	R	40	−19	7	9.12	47
Amygdala	L	−28	3	−21	8.28	9
Lingual	L	−15	−37	−2	8.07	32
Insula	R	39	−6	12	7.91	5
Insula	L	−39	−7	10	7.86	12
PHG	R	24	−33	−6	7.58	5
ACC	L/R	0	21	21	7.54	10
Putamen	L	−21	8	3	7.53	18
MCC	L	−9	12	34	7.28	12
HS > MCI						
Hippocampus	L	−34	−28	−9	10.21	35
Thalamus	R	8	−18	15	7.55	6
Caudate	R	10	6	10	7.45	13
Thalamus	L	−4	−16	15	7.13	8

k = cluster size; STG = superior temporal gyrus; Caudate = caudate nucleus; Lingual = lingual gyrus; PHG = parahippocampal gyrus; ACC/MCC = anterior/midcingulate cortex; L = left; R = right.

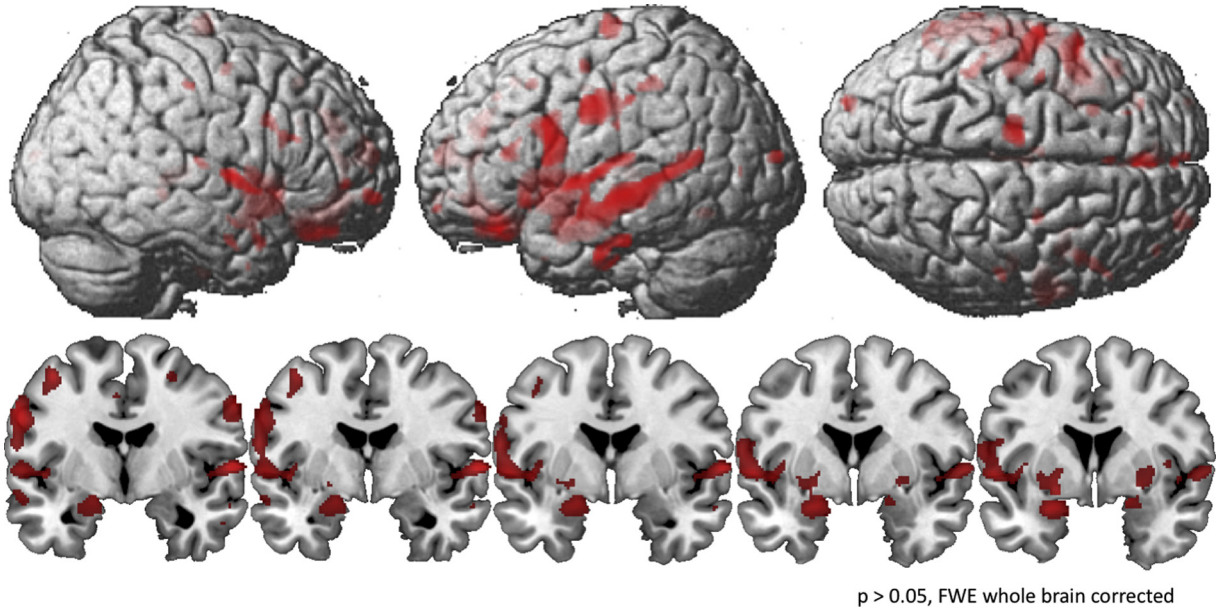

Fig. 2. Areas of reduced gray matter volume (GMV) revealed by an ANOVA (factor group), whole brain and coronal view. GMV was quantified using voxel-based morphometry (VBM) and comparisons between groups were threshold of $p < 0.05$, corrected for Family-wise Error (FWE) at whole-brain-level.

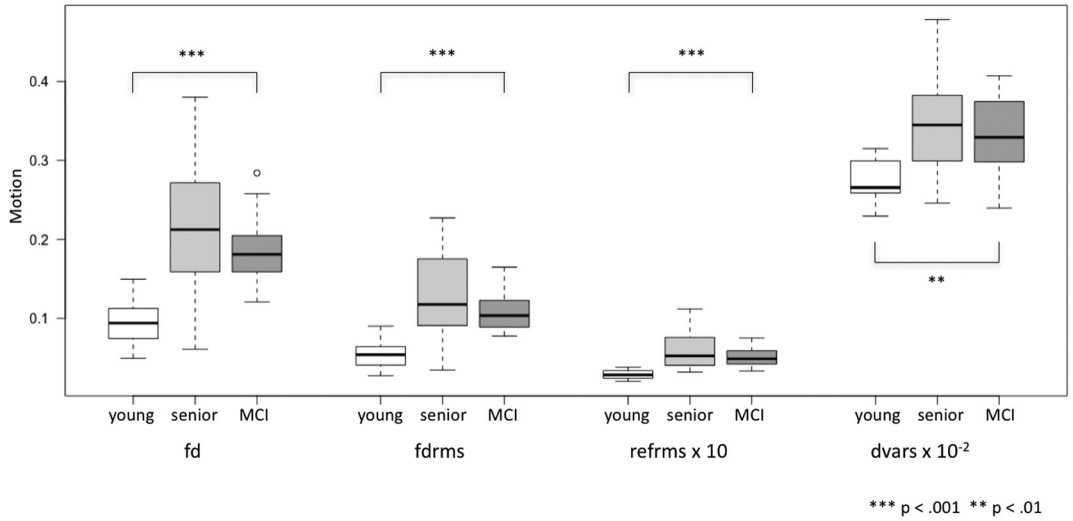

Fig. 3. Boxplots depicting motion utilizing different algorithms (fd = framewise displacement; fdrms = fd root mean square; refrms = root mean square intensity differences of volume n to the reference volume; dvars = *d* referring to temporal derivative of time courses, *vars* referring to root mean square variance over voxels). Group comparisons analyzed by an ANOVA (factor group).

all four metrics at $p \leq 0.001$, with the exception of dvars for young versus MCI, $p = 0.002$. No significant difference was found between HS and MCI (fd: $p = 0.351$; fdrms: $p = 0.237$; refrms: $p = 0.395$; dvars: $p = 0.576$).

3.5. Test-retest (TRT) reliability

ICCs were calculated voxel-wise within each group. Respective maps exhibit ICC-values in the range from 0.34 to 0.53 (see Figs. 4–5). In all groups, ICC-values varied between regions and RSN (see Table 5). The highest ICC-values were seen in the young group (see Fig. 4a), whereas ICC-values of the HS- (see Fig. 4b) and MCI-group (see Fig. 4c) were slightly lower.

3.6. Comparison of variance between groups

The comparison of intersession variance in functional connectivity between groups and voxels revealed one cluster of differing variance at a statistical level of $p < 0.05$ FWE-corrected at whole brain level. Increased variance in MCI in comparison to the young group was observed in the left caudate nucleus of the salience network (148 voxels)

When the significance level was set less stringently at $p < 0.05$ FWE-corrected at the cluster level, several additional significant clusters appeared. Specifically, MCI showed increased variance in the left caudate nucleus of the SN, in comparison to both the young and the healthy senior groups. Interestingly, the highest amount of differences in variance between groups was found in the ECN components, with increased variance in MCI compared to the other groups in the lateral PFC, cerebellum, gyrus rectus, and all three temporal gyri (ITG, MTG, STG). Increased variance in HS was limited to one cluster within the cerebellum in the ECN. No difference of variance between groups was found in the DMN. The group of young subjects exhibited no clusters of increased variance in any IC at the FWE-corrected significance level.

At a significance level of $p < 0.001$ (uncorrected, cluster extent threshold of 10 voxels), the number of clusters with higher variance in HS and MCI relative to young, increased and were found within all IC. Furthermore, differences were found when comparing HS and MCI with each other and the young group also showed a cluster of increased variance (see Table 6).

3.7. Voxel-wise correlation between variance of functional connectivity and atrophy/biomarkers/time gap/motion between sessions

To assess the association of GMV loss, biomarkers, the time gap between sessions and motion on intersession variance seperately, correlation analyses were performed. Correlations between variance and GMV loss failed to achieve significance when corrected for FWE $p < 0.05$ at both cluster and whole brain level. In contrast, significant correlations were found in all three resting state networks at a statistical level of $p < 0.001$, uncorrected, with a cluster extent threshold of 10 voxels. Areas with significant correlation between atrophy and connectivity variance included the right lateral and dorsomedial PFC, left ventromedial PFC, left ITG and MTG, as well as the right insula of the ECN. Significant correlations were also revealed in the right lateral PFC of the DMN and the left lateral PFC, precuneus, and left SFG of the SN (see Table 7).

Areas with significant correlations between cerebrospinal fluid based biomarkers (mainly phospho-tau) and connectivity variance were observed in different parts of all networks (see Table 8). Cluster-corrected significant correlations were seen only in the executive networks for phospho-tau. Areas involved were the right precuneus, left IPG, left and right MTG, and the cerebellum.

Correlations between variance and the time gap between sessions failed to achieve significance when corrected for FWE $p < 0.05$ at both cluster and whole brain level. Significant correlations were only found uncorrected for multiple comparisons ($p < 0.001$, cluster extent threshold of 10 voxels), mainly in the anterior DMN (see Table 9).

Correlations between variance and motion were also found in all three RSNs at a statistical level of $p < 0.001$, uncorrected, with a cluster extent threshold of 10 voxels. These correlations were more pronounced and frequent than between atrophy, biomarkers and the time between sessions and variance. Using a more conservative threshold ($p < 0.05$ FWE-corrected at cluster level), correlations were noted between variance and three out of four motion parameters (fd, fdrms, refrms) in the right lateral PFC of the ECN, and between refrms and variance in the cerebellum of the same network. A similar correlation was found in the cerebellum of the SN. At $p < 0.05$ FWE-corrected at whole brain level, two clusters of correlation were found between refrms and variance, one within right lateral PFC, and the other in the left MTG of the DMN (see Table 10).

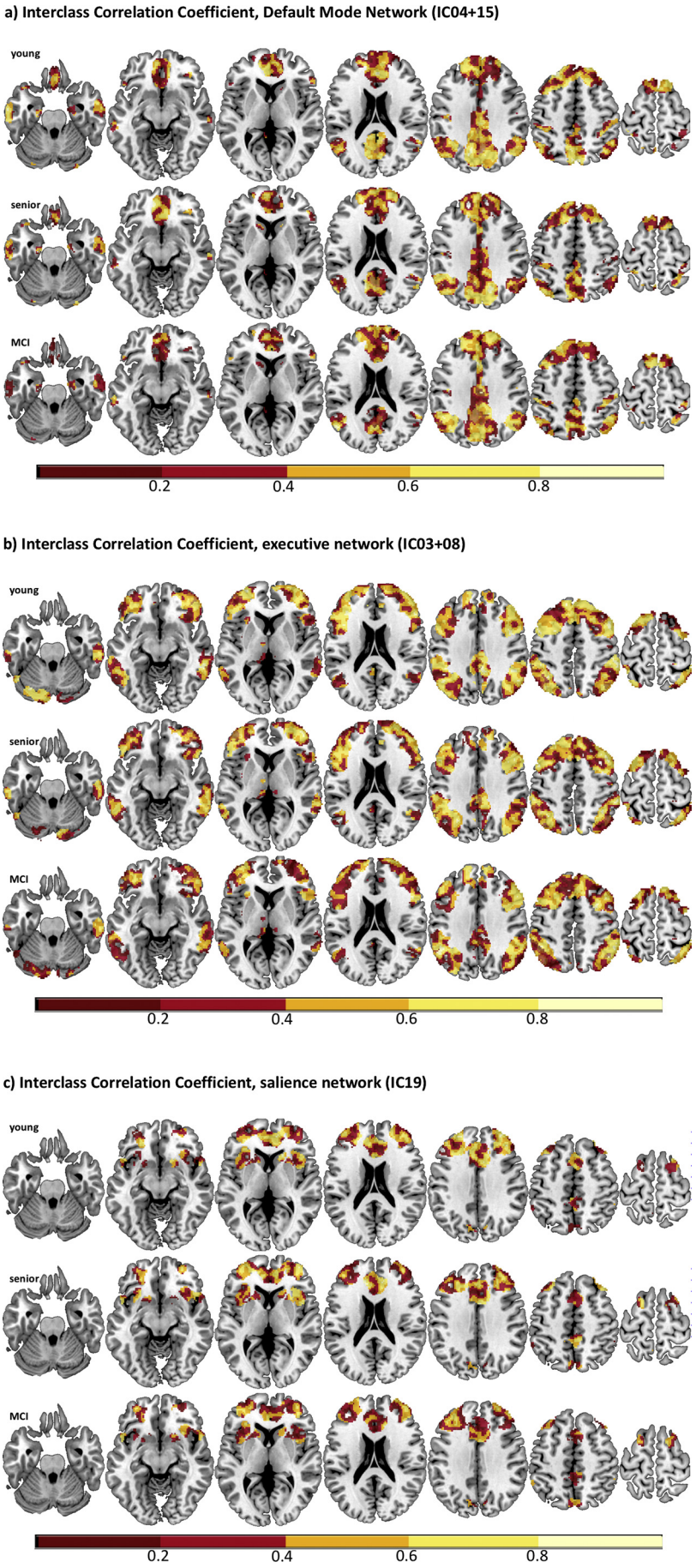

Fig. 4. a–c. Voxel-wise intraclass correlation coefficients across 3 sessions depicted for the young (upper row), senior (middle row), and the MCI group (lower row) for a) default mode network, b) executive control network, and c) salience network.

4. Discussion

We investigated the test-retest (TRT) reliability of three memory-related resting state networks (RSN), namely the Default-Mode Network (DMN), Salience Network (SN), and Executive Network (ECN), across three separate scanning sessions in young subjects, healthy seniors (HS), and patients with MCI showing evidence of AD pathology (CSF or amyloid-PET). Consistent with previous studies, overall TRT reliability between sessions was fair to moderate, with ICCs ranging from 0.34 to 0.53 (Damoiseaux et al., 2006; Chen et al., 2008; Shehzad et al., 2009; Meindl et al., 2010; Guo et al., 2012; Blautzik et al., 2013). Also in line with previous studies, ICCs were generally higher in younger subjects than in HS and MCI. Blautzik et al. reported overall moderate TRT reliability with significantly higher ICC values in HS than in MCI (HS: DMN 0.52; ECN 0.5, MCI: DMN 0.38; ECN 0.43) (Blautzik et al., 2013). Another study found fair ICC values for the DMN in young subjects (ICC 0.32) (Shehzad et al., 2009). Of the three RSN in our study, the ECN showed the greatest variance across groups with the highest ICC values obtained in the ECN of the young group, and the lowest in the ECN of the MCI group. Another finding of our study was that ICCs in more posterior brain regions were generally higher for all groups than those obtained in more frontal brain regions. This has also been observed in previous studies (Damoiseaux et al., 2008; Guo et al., 2012; Blautzik et al., 2013) and seems to especially apply to young subjects with particularly high TRT reliability, specifically in the precuneus/PCC, inferior parietal lobe, and temporal lobe (Meindl et al., 2010; Zuo et al., 2010). Differences observed in these studies when compared to ours likely stem from the diverse analytical strategies implemented, such as bootstrapping (Damoiseaux et al., 2006), comparison of size of activated areas and overlapping voxels (Meindl et al., 2010), and ICC calculation (Shehzad et al., 2009; Zuo et al., 2010; Guo et al., 2012; Blautzik et al., 2013). Other possible explanations for the incongruence of results are varying group compositions especially concerning age and disease, methods to eliminate motion, and the time gap between each measurement.

Applying an exploratory approach, the number of clusters in our intersession variance of FC analysis varied depending on the statistical threshold that was applied. Implementing a stringent level of significance ($p < 0.05$ FWE-corrected at whole brain level), only one cluster of difference in variance of FC was found in the SN between MCI and young. At a more liberal statistical level ($p < 0.05$ FWE corrected at cluster level), increased variance was mainly found in MCI compared to young in the ECN. Interestingly, no differences in variance were found within the DMN between groups at both cluster and whole brain level corrected for FWE. This might indicate a higher reliability of the DMN relative to the SN and ECN. The young group exhibited no clusters of variance at either of the FWE corrected significance levels, demonstrating particularly high TRT reliability compared to the HS and MCI. At the lowest statistical level applied in this study ($p < 0.001$, uncorrected), a criterion frequently implemented in resting state network studies, the young group exhibited a cluster of significantly greater intersession variance compared to HS and MCI. As young subjects are expected to show no increased variance when compared to the other two groups, these findings strongly suggest that the selection of this low statistical level may result in false positive findings. As a consequence, based upon our data, we suggest that in future studies of RS-FMRI a significance level of $p < 0.05$, corrected for FWE at the whole brain level, would be reasonable. However, this threshold needs to be adjusted according to individual study design, sample size, and (a priori) hypotheses.

In a next step, we investigated the influence of different confounders on the stability of RSN. Whereas the effect of the time gap between sessions was rather weak, the cerebralspinal fluid based biomarkers seem to have an effect within the MCI group. Interestingly, increasing phospho-tau values correlated with increased variability especially in the executive networks, whereas amyloid beta 42 and total-tau only showed a slight effect. This corroborates the finding that phopsho-tau indicates disease progression in Alzheimers far more than amyloid beta

Table 5
Test-retest (TRT) reliability – Voxel-wise intraclass correlation coefficients (ICC).

Resting-state network	Group	Mean ICC	Standard deviation
A. Anterior DMN	Young	0.40	0.23
	Healthy seniors	0.35	0.24
	MCI	0.36	0.23
B. Posterior DMN	Young	0.53	0.23
	Healthy seniors	0.36	0.25
	MCI	0.42	0.24
C. Salience Network	Young	0.41	0.24
	Healthy seniors	0.38	0.23
	MCI	0.34	0.23
D. Executive Control (right)	Young	0.46	0.23
	Healthy seniors	0.39	0.24
	MCI	0.36	0.23
E. Executive Control (left)	Young	0.48	0.22
	healthy seniors	0.46	0.23
	MCI	0.34	0.23

Intersession test-retest reliability was evaluated by intraclass correlation coefficient (ICC) comparisons. ICC-values varied between regions and resting- state networks, as well as groups.

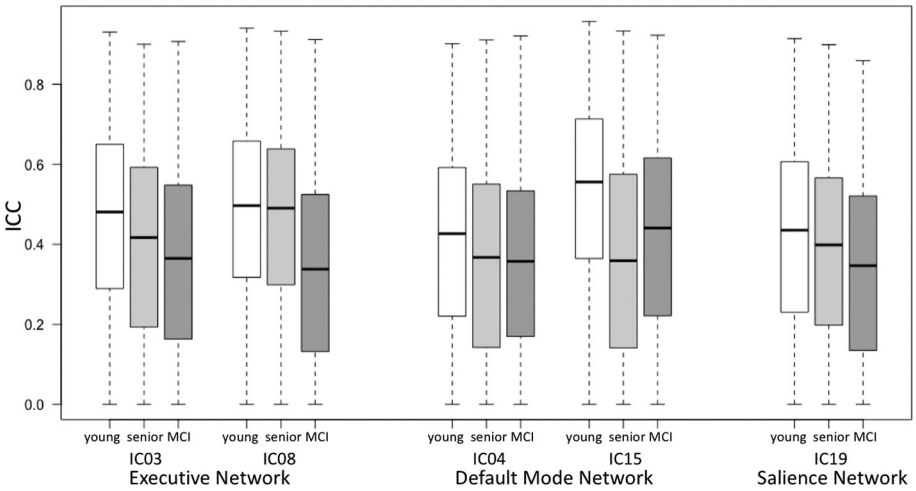

Fig. 5. Boxplots depicting mean ICC for the different groups and resting-state networks separately (ICC = intraclass correlation coefficient; IC = independent component).

Table 6
Differences in intersession variance of functional connectivity between groups.

Comparison between groups	Region	Side
A. Anterior DMN		
MCI > HS	–	–
MCI > young	Temporal Pole	L
	SFG	L
	Olfactory	R
HS > MCI	–	–
HS > young	SFG	R
young > MCI	–	–
young > HS	IPL (supramarginal gyrus)	L
B. Posterior DMN		
MCI > HS	–	–
MCI > young	SFG	R
	Thalamus	L
	IPG	R
HS > MCI	IPG	L
HS > young	MTG	R
	Precuneus	R
	IPL (angular gyrus)	L
	MCC	R
young > MCI	–	–
young > HS	–	–
C. Salience Network		
MCI > HS	Caudate*	L
	Caudate	R
MCI > young	Caudate*,**	L
	Caudate	R
	Insula	L
	lPFC	L
	lPFC	R
HS > MCI	–	–
HS > young	Cerebellum	R
	vlPFC	L
	SFG	R
	dmPFC	L
young > MCI	–	–
young > HS	–	–
D. Executive Control (right)		
MCI > HS	lPFC	R
	STG	R
MCI > young	lPFC*	R
	STG*	R
	Insula	R
	Caudate	R
	Olfactory	R
	Cerebellum	L
	IPL (angular gyrus)	L
	ITG	L
	ACC	R
	MCC	R
	dmPFC	R
	SPR	R
	dlPFC	R
HS > MCI	–	–
HS > young	Precuneus	R
	dmPFC	R
	lPFC	R
	Cerebellum*	L
	SFG	R
	MCC	R
	IPL (angular gyrus)	L
	IPL (supramarginal gyrus)	R
	SPR	L
	vmPFC	L
	Caudate	R
young > MCI	–	–
young > HS	–	–
E. Executive Control (left)		
MCI > HS	Gyrus rectus	L
MCI > young	IPL (angular gyrus)	R
	Cerebellum*	R
	ITG	L
	Gyrus rectus*	L
	vmPFC	L
	ITG*	R
	MTG*	R
	lPFC	R
	vlPFC	L
	Insula	L
	Thalamus	L
HS > MCI	–	–
HS > young	IPL (angular gyrus)	R
	SFG	L
	MOG	L
	dmPFC	L
young > MCI	–	–
young > HS	–	–

The comparison of connectivity variance (group mean square) between groups within the ICs was conducted performing an ANOVA. Three levels of height thresholds were applied (i. uncorrected $p < 0.001$; *$p < 0.001$ to form clusters considered significant at cluster level $p < 0.05$ FWE-corrected; ** FWE-corrected $p < 0.05$ on a whole-brain-level) and clusters were required to consist of at least 10 voxels each. The more liberal the threshold, the more clusters with higher variance in HS and MCI relative to young appeared. SPR = superior parietal region; SFG = superior frontal gyrus; IPL = inferior parietal lobe; IPG = inferior parietal gyrus; ITG/ MTG = inferior/ medial temporal gyrus; ACC/ MCC = anterior/ mid cingulate cortex; l/dm/dl/vm/vl PFC = lateral, dorsomedial, dorsolateral, ventromedial, ventrolateral prefrontal cortex; rectus = gyrus rectus; MOG = middle occipital gyrus; L = left; R = right.

Table 7
Correlation of variance in functional connectivity and atrophy.

Resting-state network	Region	Side	k	FWE cluster	FWE whole brain
A. Anterior DMN	lPFC	R	11	0.997	0.916
B. Posterior DMN	–	–		–	–
C. Salience Network	Precuneus	L	21	0.967	0.955
	SFG	L	13	0.994	0.978
	lPFC	L	13	0.994	0.996
D. Executive Control (right)	Insula	R	17	0.984	0.278
	MTG	L	28	0.918	0.815
	ITG	L	28	0.918	0.963
	dmPFC	R	20	0.972	0.851
	lPFC	R	10	0.998	0.995
E. Executive Control (left)	vmPFC	L	12	0.995	0.125

A voxel-wise correlation between variance of functional connectivity within the respective ICs and VBM maps was performed to compute correlation values between variance and cortical atrophy. Significant correlations in the respective resting state networks at a statistical level of $p < 0.001$ (uncorrected and a cluster extent of 10 voxels) are listed. Additionally, FWE cluster corrected and FWE whole brain corrected values are presented. l/dm/vm PFC = lateral, dorsomedial, ventromedial prefrontal cortex; SFG = superior frontal gyrus; ITG/ MTG = inferior/ medial temporal gyrus; L = left; R = right.

42 (Giacobini and Gold, 2013) and implies that our findings of group differences are realted to the underlying disease.

Another confounder that may be associated with alterations of resting state brain activity is local atrophy (Johnson et al., 2000; Kalpouzos et al., 2012). Previous studies that looked at the effect of atrophy correction on FC found mixed results. One study reported that not all regions of connectivity changes survived atrophy correction (Binnewijzend et al., 2012), while other studies observed that all results remained unchanged (Bai et al., 2008; Agosta et al., 2012), or maintained their statistical significance but experienced a decrease of statistical power (He et al., 2007). In line with previous studies, the HS and

Table 8
Correlation of variance in functional connectivity and biomarkers.

Resting-state network	Region	Biomarker	Side	k	FWE cluster	FWE whole brain
A. Anterior DMN	ACC	PTAU	L	13	0.758	1.000
	Precuneus	TAU	R	19	0.324	1.000
	Caudate	TAU	L	16	0.519	1.000
	Angular gyrus	TAU	L	15	0.597	1.000
B. Posterior DMN	Precuneus	PTAU	L	14	0.683	0.851
	Cuneus	PTAU	L	10	0.948	0.999
	PCC	PTAU	R	22	0.197	1.000
	Precuneus	PTAU	R	19	0.328	1.000
	Precuneus	PTAU	L	15	0.602	1.000
	MTG	PTAU	R	14	0.683	1.000
	IPL	TAU	L	17	0.450	1.000
	MCC	TAU	R	13	0.763	1.000
C. Salience Network	Precuneus	Aß42	R	11	0.899	1.000
	Lingual	PTAU	L	12	0.835	0.995
	IPG	PTAU	L	15	0.598	0.999
	Precuneus	PTAU	R	17	0.447	1.000
	SFG	PTAU	R	14	0.679	1.000
D. Executive Control (right)	Precuneus	Aß42	R	16	0.521	1.000
	Precuneus	PTAU	R	147	0.000	0.849
	Cerebellum	PTAU	L	34	0.025	0.891
	IPG	PTAU	L	71	0.000	0.997
	IPG	PTAU	L	11	0.900	0.999
	vlPFC	PTAU	R	15	0.599	1.000
	MCC	PTAU	R	14	0.681	1.000
	MCC	PTAU	R	16	0.521	1.000
	SPR	PTAU	R	16	0.521	1.000
	MTG	PTAU	R	41	0.008	1.000
	IPL (supramarg.)	PTAU	R	11	0.900	1.000
	dlPFC	PTAU	R	11	0.900	1.000
	MTG	PTAU	R	20	0.275	1.000
E. Executive Control (left)	MTG	PTAU	L	32	0.029	0.999
	dlPFC	PTAU	L	13	0.733	1.000
	MOG	PTAU	L	10	0.937	1.000
	MTG	PTAU	R	10	0.937	1.000
	IOG	PTAU	L	21	0.207	1.000
	Cerebellum	PTAU	R	17	0.414	1.000
	MCC	TAU	L/R	17	0.417	1.000

A voxel-wise correlation between variance of functional connectivity within the respective ICs and biomarkers was performed to compute correlation values between variance and cerebrospinal fluid based biomarkers. Significant correlations in the respective resting state networks at a statistical level of $p < 0.001$ (uncorrected and a cluster extent of 10 voxels) are listed. Additionally, FWE cluster corrected and FWE whole brain corrected values are presented. ACC/ MCC/ PCC = anterior / mid/ posterior cingulate cortex; MTG = medial temporal gyrus; Lingual = lingual gyrus; IPG = inferior parietal gyrus; SFG = superior frontal gyrus; dl/ vlPFC = dorsolateral/ ventrolateral prefrontal cortex; SPR = superior parietal regions; IPL = inferior parietal lobe; MOG/ IOG = middle/ inferior occipital gyrus; Aß42 = Amyloid-Beta 42; PTAU = Phospho-Tau-Protein; TAU = Tau-Protein.

MCI subjects of our study showed significantly reduced GMV compared to young subjects in several brain regions that are part of the RSN of interest. This holds especially true for regions within the temporal lobe (Sorg et al., 2007; Fjell et al., 2009). Correlating the intersession variance of FC and atrophy voxel-wise, we found significant correlations, consistent in all three RSN, in the frontal areas of the brain but not in the hippocampus, the area with the most prominent difference in GMV between HS and MCI subjects. On one hand, these findings are in line with previous studies that showed reduced FC in frontal regions in HS and suggested atrophy as a possible origin (Damoiseaux et al., 2008; Huang et al., 2015; Marchitelli et al., 2016). On the other hand, this discrepancy raises questions regarding the influence of atrophy on functional connectivity. The conclusion of a mere decreasing of FC with advancing neuronal loss can not be drawn (Joo et al., 2016; Serra et al., 2016). Taking the forementioned mixed previous results into account, our findings imply that an correction for atrophy can not be recommended in general terms and needs to be considered carefully, as it might mask relevant results.

Table 9
Correlation of variance in functional connectivity and time gap between sessions.

Resting-state network	Region	Side	k	FWE cluster	FWE whole brain
A. Anterior DMN	IPL (angular gyrus)	R	33	0.326	0.295
	Lingual	R	11	0.996	0.779
	MTG	R	16	0.939	0.820
	PCC	L	44	0.125	0.953
	dmPFC	L	16	9.939	0.992
	Precuneus	L	12	0.992	0.998
	Postcentral gyrus	R	22	0.734	1.000
	MTG	R	10	0.999	1.000
B. Posterior DMN	MCC	R	32	0.353	0.878
C. Salience Network	vlPFC	L	13	0.986	0.905
	dmPFC	R/L	11	0.997	1.000
	Cuneus	R	18	0.889	1.000
D. Executive Control (right)	dlPFC	R	14	0.975	0.467
E. Executive Control (left)	–	–	–	–	–

A voxel-wise correlation between variance of functional connectivity within the respective ICs and timimg parameters as performed to compute correlation values between variance and the time gap between sessions. Significant correlations in the respective resting state networks at a statistical level of $p < 0.001$ (uncorrected and a cluster extent of 10 voxels) are listed. Additionally, FWE cluster corrected and FWE whole brain corrected values are presented. IPL = inferior parietal lobe; Lingual = lingual gyrus; MTG = medial temporal gyrus; MCC/ PCC = mid/ posterior cingulate cortex; dm/ dl/ vlPFC = dorsomedial/ dorsolateral/ ventrolateral prefrontal cortex.

Finally, a factor known to influence functional connectivity is motion (Van Dijk et al., 2012; Power et al., 2015). In this study, both the HS subjects and those with MCI exhibited significantly increased motion compared to the young subjects. It is widely acknowledged that in an MRI scanner, HS and MCI tend to move more than young adults. In order to assess the degree of influence motion had, we correlated the variance in intersession FC with motion parameters. Results showed that correlations for motion were far more pronounced and frequent than for atrophy, biomarkers and the time gap between the sessions. Although the amount of head movement found in our study was within normal ranges, it showed a marked impact on the reliability of FC. Even at the most conservative significance level ($p < 0.05$, corrected for FWE at whole brain level), clusters of significant correlations of FC with motion were found within the DMN. In a recent study, Marchitelli et al. conducted a bivariate Pearson's correlation to examine the relationship between TRT reliability of the DMN and motion across two sessions in HE (Marchitelli et al., 2016). Different to our approach, they only examined the motion parameter fd and only invoked the stringent statistical criterion of $p < 0.05$. The differing analysis renders a comparison with our results difficult. However, their findings of significant anti-correlations between the Jaccard index for DMN across sessions and motion corroborate our observation, that TRT reliability is significantly lowered by motion. In summary, the overall lower TRT reliability in MCI and HS, represented both by lower ICCs and higher intersession variance, can be, at least in part, explained by the influence of motion.

The following limitations need to be discussed: We cannot fully preclude that participants fell asleep during the scans. However, participants were asked to fill out a fatigue questionnaire and were observed via a camera while lying in the MR scanner. In addition, healthy seniors were not subjected to lumbar punctures or amyloid PET scans. There is therefore a possibility that healthy senior subjects in this study might have been affected by amyloid deposition (Brier et al., 2014). As only one resting-state-run was applied in one session, we do not know if the effects demonstrated above are also present when acquiring resting-

state data from subsequent runs. Further, we do not know how multiple sessions could contribute to a more stable network signal. As a next step towards establishing resting-state networks as imaging-based biomarkers, future research should investigate whether the variability between sessions found in this study persists when measuring multiple runs within each session so as to quantify the between-session variability. Finally, Biswal et al. found that results obtained with a small sample size (e.g. 50 subjects) might lead to false negative results (Biswal et al., 2010). The number of subjects chosen to participate in this study is consistent with many other studies performing RS fMRI, therefore we provide further evidence on reliability for studies with similar designs and number of subjects. However, these results should be replicated with larger sample sizes.

To conclude, this study provides important insights into the reliability of RSN involving groups vulnerable to increased variance due to functional, structural and biochemical changes. Overall, fair to moderate reliability was found across groups and sessions. As concrete recommendations derived from our results we suggest, that stringent statistical thresholds should be applied when assessing the value of RSN as biomarkers in neurodegenerative diseases. Our study also sheds light on the impact of motion as a major confounder influencing variance in FC between RS fMRI sessions. By utilizing sophisticated motion correction algorithms in the preprocessing-step and adding motion as a covariate in the models in the future, the TRT realiability can be increased. For subject groups with Alzheimer pathology, cerebralspinal fluid based biomarkers should be used as a covariate. In this context it seems that phospho-tau has an higher impact than amyloid beta 42 and total-tau. In respect to GMV loss, a clear recommendation without ambiguity is difficult, as including GMV loss as a covariate might mask biologically interesting results. Taken into account that the effects of atrophy on variability are limited in comparison to e.g. motion, and we in any case recommend stringent thresholds, this covariate could be

Table 10
Correlation of variance in functional connectivity and motion.

Resting-state network	Motion parameter	Region	Side	k	0.001 uncor.	FWE cluster	FWE whole brain
A. Anterior DMN	dvars	SPR	L	19	+	−	−
	fd	IPL (angular gyrus)	L	13	+	−	−
		SFG	L	14	+	−	−
		Temporal Pole	R	11	+	−	−
	fdrms	IPL (angular gyrus)	L	14	+	−	−
		SFG	L	16	+	−	−
		SFG	R	10	+	−	−
		Temporal Pole	R	14	+	−	−
	refrms	Fusiform gyrus	L	13	+	−	−
		SFG	R	14	+	−	−
		SPR	L	10	+	−	−
		Caudate	L	14	+	−	−
		IPL (angular gyrus)	R	21	+	−	−
		SPR	R	14	+	−	−
B. Posterior DMN	dvars	MTG	R	24	+	−	−
		MTG	L	17	+	−	−
	fd	ITG	L	15	+	−	−
		MTG	R	11	+	−	−
		IPL (angular gyrus)	L	10	+	−	−
		IPL (angular gyrus)	R	23	+	−	−
		MTG	L	26	+	−	−
		Temporal Pole	R	10	+	−	−
	fdrms	MTG	R	11	+	−	−
		ITG	L	13	+	−	−
		IPL (angular gyrus)	R	21	+	−	−
		MTG	L	21	+	−	−
		IPL (angular gyrus)	L	31	+	−	−
	refrms	lPFC	R	27	+	−	+
		MTG	L	48	+	−	+
		MTG	R	16	+	−	−
		SOG	L	15	+	−	−
		IPG	R	29	+	−	−
		IPL (angular gyrus)	L	15	+	−	−
C. Salience Network	dvars	Cerebellum	L	33	+	−	−
		Cerebellum	R	41	+	−	−
		SFG	R	16	+	−	−
		lPFC	L	19	+	−	−
	fd	Cerebellum	R	30	+	−	−
		SFG	R	30	+	−	−
		Temporal Pole	R	16	+	−	−
		lPFC	L	36	+	−	−
		SPR	R	20	+	−	−
	fdrms	Cerebellum	R	34	+	−	−
		SFG	R	10	+	−	−
		Temporal Pole	R	17	+	−	−
		ACC	R	11	+	−	−
		lPFC	L	30	+	−	−
		SPR	R	19	+	−	−
	refrms	Cerebellum	R	87	+	+	−
		SFG	R	34	+	−	−
		dmPFC	R	34	+	−	−
		Cerebellum	L	33	+	−	−
		lPFC	L	22	+	−	−

(*continued on next page*)

Table 10 (*continued*)

Resting-state network	Motion parameter	Region	Side	k	0.001 uncor.	FWE cluster	FWE whole brain
D. Executive Control (right)	dvars	IPG	L	11	+	−	−
		dmPFC	R	26	+	−	−
		SPR	R	13	+	−	−
		Cerebellum	L	10	+	−	−
		lPFC	R	27	+	−	−
		IPL	L	10	+	−	−
		dmPFC	L	16	+	−	−
		Thalamus	R	26	+	−	−
	fd	lPFC	R	88	+	+	−
		Cerebellum	L	42	+	−	−
		IPL (angular gyrus)	R	19	+	−	−
		SFG	R	37	+	−	−
		dmPFC	R	37	+	−	−
		dlPFC	R	11	+	−	−
		MCC	R	11	+	−	−
		IPG	L	15	+	−	−
		SPR	R	13	+	−	−
		ITG	L	10	+	−	−
	fdrms	lPFC	R	95	+	+	−
		Cerebellum	L	46	+	−	−
		IPL (angular gyrus)	R	18	+	−	−
		SFG	R	35	+	−	−
		dmPFC	R	35	+	−	−
		MCC	R	10	+	−	−
		lPFC	R	13	+	−	−
		Hippocampus	R	12	+	−	−
	refrms	Cerebellum	L	86	+	+	−
		lPFC	R	49	+	−	−
		IPL (supramarginal gyrus)	R	26	+	−	−
		SPR	R	12	+	−	−
		MCC	R	12	+	−	−
		IPL (angular gyrus)	R	14	+	−	−
		Thalamus	R	37	+	−	−
		SPR	L	15	+	−	−
		IPG	R	10	+	−	−
		IPG	L	10	+	−	−
		SFG	R	13	+	−	−
E. Executive Control (left)	dvars	ITG	L	18	+	−	−
		Thalamus	L	30	+	−	−
		vlPFC	L	13	+	−	−
		IPL (angular gyrus)	L	21	+	−	−
		Cerebellum	R	18	+	−	−
		lPFC	L	32	+	−	−
		dmPFC	R	18	+	−	−
		MTG	L	10	+	−	−
	fd	Thalamus	L	22	+	−	−
		MOG	L	21	+	−	−
		IPL (angular gyrus)	L	34	+	−	−
		lPFC	L	18	+	−	−
		SFG	L	18	+	−	−
	fdrms	MOG	L	28	+	−	−
		Thalamus	L	17	+	−	−
		IPL (angular gyrus)	L	35	+	−	−
		lPFC	L	26	+	−	−
	refrms	ITG	L	22	+	−	−
		MTG	L	43	+	−	−
		MTG	R	22	+	−	−
		lPFC	R	73	+	+	−
		Cerebellum	R	68	+	+	−
		IPL (angular gyrus)	L	21	+	−	−
		dlPFC	L	16	+	−	−
		Thalamus	L	14	+	−	−
		dmPFC	L	22	+	−	−

Correlations between variance and motion were found in all three RSNs at a statistical level of with $p < 0.001$, uncorrected and a cluster extent threshold of 10 voxels, some of them were also found at more conservative thresholds. SPR = superior parietal regions; IPL = inferior parietal lobe; SFG = superior frontal gyrus; Caudate = caudate nucleus; ITG/ MTG = inferior/ medial temporal gyrus; SOG/ MOG = superior/ middle occipital gyrus; IPG = inferior parietal gyrus; ACC/ MCC/ PCC = anterior/ mid/ posterior cingulate cortex; Dm/dlvl PFC = dorsomedial, dorsolateral, ventrolateral prefrontal cortex; L = left; R = right.

omitted in concordance with the research question. This is particulary applicable for repeated measures within subjects. And finally, reliability is partly influenced by the time gap between repeated measurements. To diminish the influence of this confounder we recommend to keep the time gap between measurements as constant as possible. Following these recommendations, variability could be decreased and, hence, sensitivity and specificity increased. If these recommendations are not applied, one should be cautious with subsequent inferences.

Financial interests or conflicts of interest

The authors have no conflicts of interest to report, nor any involvement to disclose, financial or otherwise, that may bias the conduct, interpretation, or presentation of this work.

Declarations of interest

None.

Funding

OAO was supported by the Koeln Fortune Program/Faculty of Medicine, University of Cologne (217/2011) and the Brandau-Laibach-Foundation. GRF, OAO and JK are grateful for the support of the Marga- and Walter-Boll-Foundation. This research did not receive any specific grant from funding agencies in the commercial sectors.

Acknowledgements

All authors wish to thank Nina Nolfo and Stefan Metzger for their assistance in data collection.

References

Agosta, F., Pievani, M., Geroldi, C., Copetti, M., Frisoni, G.B., Filippi, M., 2012. Resting state fMRI in Alzheimer's disease: beyond the default mode network. Neurobiol. Aging 33, 1564–1578.
Ashburner, J., Friston, K.J., 2000. Voxel-based morphometry—the methods. NeuroImage 11, 805–821.
Bai, F., Zhang, Z., Yu, H., Shi, Y., Yuan, Y., Zhu, W., Zhang, X., Qian, Y., 2008. Default-mode network activity distinguishes amnestic type mild cognitive impairment from healthy aging: a combined structural and resting-state functional MRI study. Neurosci. Lett. 438, 111–115.
Barkhof, F., Haller, S., Rombouts, S.A., 2014. Resting-state functional MR imaging: a new window to the brain. Radiology 272, 29–49.
Beckmann, C.F., Deluca, M., Devlin, J.T., Smith, S.M., 2005. Investigations into resting-state connectivity using independent component analysis. Philos. Trans. R. Soc. Lond. Ser. B Biol. Sci. 360, 1001–1013.
Binnewijzend, M.A., Schoonheim, M.M., Sanz-Arigita, E., Wink, A.M., van der Flier, W.M., Tolboom, N., Adriaanse, S.M., Damoiseaux, J.S., Scheltens, P., van Berckel, B.N., Barkhof, F., 2012. Resting-state fMRI changes in Alzheimer's disease and mild cognitive impairment. Neurobiol. Aging 33, 2018.
Biswal, B., Yetkin, F.Z., Haughton, V.M., Hyde, J.S., 1995. Functional connectivity in the motor cortex of resting human brain using echo-planar MRI. Magn. Reson. Med. 34, 537–541.
Biswal, B.B., Mennes, M., Zuo, X.N., Gohel, S., Kelly, C., Smith, S.M., Beckmann, C.F., Adelstein, J.S., Buckner, R.L., Colcombe, S., Dogonowski, A.M., Ernst, M., Fair, D., Hampson, M., Hoptman, M.J., Hyde, J.S., Kiviniemi, V.J., Kotter, R., Li, S.J., Lin, C.P., Lowe, M.J., Mackay, C., Madden, D.J., Madsen, K.H., Margulies, D.S., Mayberg, H.S., McMahon, K., Monk, C.S., Mostofsky, S.H., Nagel, B.J., Pekar, J.J., Peltier, S.J., Petersen, S.E., Riedl, V., Rombouts, S.A., Rypma, B., Schlaggar, B.L., Schmidt, S., Seidler, R.D., Siegle, G.J., Sorg, C., Teng, G.J., Veijola, J., Villringer, A., Walter, M., Wang, L., Weng, X.C., Whitfield-Gabrieli, S., Williamson, P., Windischberger, C., Zang, Y.F., Zhang, H.Y., Castellanos, F.X., Milham, M.P., 2010. Toward discovery science of human brain function. Proc. Natl. Acad. Sci. U. S. A. 107, 4734–4739.
Blautzik, J., Keeser, D., Berman, A., Paolini, M., Kirsch, V., Mueller, S., Coates, U., Reiser, M., Teipel, S.J., Meindl, T., 2013. Long-term test-retest reliability of resting-state networks in healthy elderly subjects and with amnestic mild cognitive impairment patients. J. Alzheimers Dis. 34, 741–754.
Bowie, C.R., Harvey, P.D., 2006. Administration and interpretation of the Trail Making Test. Nat. Protoc. 1, 2277–2281.
Brier, M.R., Thomas, J.B., Snyder, A.Z., Wang, L., Fagan, A.M., Benzinger, T., Morris, J.C., Ances, B.M., 2014. Unrecognized preclinical Alzheimer disease confounds rs-fcMRI studies of normal aging. Neurology 83, 1613–1619.
Buckner, R.L., Krienen, F.M., Yeo, B.T., 2013. Opportunities and limitations of intrinsic functional connectivity MRI. Nat. Neurosci. 16, 832–837.
Calhoun, V.D., Adali, T., Pearlson, G.D., Pekar, J.J., 2001. A method for making group inferences from functional MRI data using independent component analysis. Hum. Brain Mapp. 14, 140–151.
Cha, J., Jo, H.J., Kim, H.J., Seo, S.W., Kim, H.S., Yoon, U., Park, H., Na, D.L., Lee, J.M., 2013. Functional alteration patterns of default mode networks: comparisons of normal aging, amnestic mild cognitive impairment and Alzheimer's disease. Eur. J. Neurosci. 37, 1916–1924.
Chen, S., Ross, T.J., Zhan, W., Myers, C.S., Chuang, K.S., Heishman, S.J., Stein, E.A., Yang, Y., 2008. Group independent component analysis reveals consistent resting-state networks across multiple sessions. Brain Res. 1239, 141–151.
Chou, Y.H., Panych, L.P., Dickey, C.C., Petrella, J.R., Chen, N.K., 2012. Investigation of long-term reproducibility of intrinsic connectivity network mapping: a resting-state fMRI study. AJNR Am. J. Neuroradiol. 33, 833–838.
Cole, D.M., Smith, S.M., Beckmann, C.F., 2010. Advances and pitfalls in the analysis and interpretation of resting-state FMRI data. Front. Syst. Neurosci. 4, 8.
Damoiseaux, J.S., Rombouts, S.A., Barkhof, F., Scheltens, P., Stam, C.J., Smith, S.M., Beckmann, C.F., 2006. Consistent resting-state networks across healthy subjects. Proc. Natl. Acad. Sci. U. S. A. 103, 13848–13853.
Damoiseaux, J.S., Beckmann, C.F., Arigita, E.J., Barkhof, F., Scheltens, P., Stam, C.J., Smith, S.M., Rombouts, S.A., 2008. Reduced resting-state brain activity in the "default network" in normal aging. Cereb. Cortex 18, 1856–1864.
Deichmann, R., Gottfried, J.A., Hutton, C., Turner, R., 2003. Optimized EPI for fMRI studies of the orbitofrontal cortex. NeuroImage 19, 430–441.
Dickerson, B.C., Sperling, R.A., 2005. Neuroimaging biomarkers for clinical trials of disease-modifying therapies in Alzheimer's disease. NeuroRx 2, 348–360.
Dubois, B., Feldman, H.H., Jacova, C., Hampel, H., Molinuevo, J.L., Blennow, K., DeKosky, S.T., Gauthier, S., Selkoe, D., Bateman, R., Cappa, S., Crutch, S., Engelborghs, S., Frisoni, G.B., Fox, N.C., Galasko, D., Habert, M.O., Jicha, G.A., Nordberg, A., Pasquier, F., Rabinovici, G., Robert, P., Rowe, C., Salloway, S., Sarazin, M., Epelbaum, S., de Souza, L.C., Vellas, B., Visser, P.J., Schneider, L., Stern, Y., Scheltens, P., Cummings, J.L., 2014. Advancing research diagnostic criteria for Alzheimer's disease: the IWG-2 criteria. Lancet Neurol. 13, 614–629.
Dubois, B., Hampel, H., Feldman, H.H., Scheltens, P., Aisen, P., Andrieu, S., Bakardjian, H., Benali, H., Bertram, L., Blennow, K., Broich, K., Cavedo, E., Crutch, S., Dartigues, J.F., Duyckaerts, C., Epelbaum, S., Frisoni, G.B., Gauthier, S., Genthon, R., Gouw, A.A., Habert, M.O., Holtzman, D.M., Kivipelto, M., Lista, S., Molinuevo, J.L., O'Bryant, S.E., Rabinovici, G.D., Rowe, C., Salloway, S., Schneider, L.S., Sperling, R., Teichmann, M., Carrillo, M.C., Cummings, J., Jack Jr., C.R., 2016. Preclinical Alzheimer's disease: definition, natural history, and diagnostic criteria. Alzheimers Dement. 12, 292–323.
Duits, F.H., Prins, N.D., Lemstra, A.W., Pijnenburg, Y.A., Bouwman, F.H., Teunissen, C.E., Scheltens, P., van der Flier, W.M., 2015. Diagnostic impact of CSF biomarkers for Alzheimer's disease in a tertiary memory clinic. Alzheimers Dement. 11, 523–532.
Erhardt, E.B., Rachakonda, S., Bedrick, E.J., Allen, E.A., Adali, T., Calhoun, V.D., 2011. Comparison of multi-subject ICA methods for analysis of fMRI data. Hum. Brain Mapp. 32, 2075–2095.
Fjell, A.M., Westlye, L.T., Amlien, I., Espeseth, T., Reinvang, I., Raz, N., Agartz, I., Salat, D.H., Greve, D.N., Fischl, B., Dale, A.M., Walhovd, K.B., 2009. High consistency of regional cortical thinning in aging across multiple samples. Cereb. Cortex 19, 2001–2012.
Folstein, M.F., Folstein, S.E., McHugh, P.R., 1975. "Mini-mental state". A practical method for grading the cognitive state of patients for the clinician. J. Psychiatr. Res. 12, 189–198.
Fox, M.D., Snyder, A.Z., Vincent, J.L., Corbetta, M., Van Essen, D.C., Raichle, M.E., 2005. The human brain is intrinsically organized into dynamic, anticorrelated functional networks. Proc. Natl. Acad. Sci. U. S. A. 102, 9673–9678.
Franco, A.R., Pritchard, A., Calhoun, V.D., Mayer, A.R., 2009. Interrater and intermethod reliability of default mode network selection. Hum. Brain Mapp. 30, 2293–2303.
Garrity, A.G., Pearlson MD, Godfrey D., PD, Kristen McKiernan, Dan Lloyd, P.D., Kiehl PD, Kent A., Calhoun PD, Vince D., 2007. Aberrant “default mode” functional connectivity in schizophrenia. Am. J. Psychiatr. 164, 450–457.
Giacobini, E., Gold, G., 2013. Alzheimer disease therapy—moving from amyloid-beta to tau. Nat. Rev. Neurol. 9, 677–686.
Goekoop, R., Rombouts, S.A., Jonker, C., Hibbel, A., Knol, D.L., Truyen, L., Barkhof, F., Scheltens, P., 2004. Challenging the cholinergic system in mild cognitive impairment: a pharmacological fMRI study. NeuroImage 23, 1450–1459.
Gomez-Ramirez, J., Wu, J., 2014. Network-based biomarkers in Alzheimer's disease: review and future directions. Front. Aging Neurosci. 6, 12.
Good, C.D., Johnsrude, I.S., Ashburner, J., Henson, R.N., Friston, K.J., Frackowiak, R.S., 2001. A voxel-based morphometric study of ageing in 465 normal adult human brains. NeuroImage 14, 21–36.
Grundman, M., Petersen, R.C., Ferris, S.H., et al., 2004. MIld cognitive impairment can be distinguished from alzheimer disease and normal aging for clinical trials. Arch. Neurol. 61, 59–66.
Guo, C.C., Kurth, F., Zhou, J., Mayer, E.A., Eickhoff, S.B., Kramer, J.H., Seeley, W.W., 2012. One-year test-retest reliability of intrinsic connectivity network fMRI in older adults. NeuroImage 61, 1471–1483.
Habas, C., Kamdar, N., Nguyen, D., Prater, K., Beckmann, C.F., Menon, V., Greicius, M.D., 2009. Distinct cerebellar contributions to intrinsic connectivity networks. J. Neurosci. 29, 8586–8594.
Hamilton, M., 1960. A rating scale for depression. J. Neurol. Neurosurg. Psychiatry 23, 56–62.
Hampson, M., Peterson, B.S., Skudlarski, P., Gatenby, J.C., Gore, J.C., 2002. Detection of functional connectivity using temporal correlations in MR images. Hum. Brain Mapp. 15, 247–262.
He, Y., Wang, L., Zang, Y., Tian, L., Zhang, X., Li, K., Jiang, T., 2007. Regional coherence changes in the early stages of Alzheimer's disease: a combined structural and resting-state functional MRI study. NeuroImage 35, 488–500.
Helmstaedter, C., Lendt, M., Lux, S., 2001. Verbaler Lern- und Merkfähigkeitstest. VLMT: Beltz-Test.
Hindmarch, I., Lehfeld, H., de Jongh, P., Erzigkeit, H., 1998. The Bayer activities of daily living scale (B-ADL). Dement. Geriatr. Cogn. Disord. 9 (Suppl. 2), 20–26.
Horn, W., 1983. Leistungsprüfsystem (LPS): Handanweisung. 2. überarbeitete und verbesserte Auflage. Hogrefe, Göttingen.
Huang, C.C., Hsieh, W.J., Lee, P.L., Peng, L.N., Liu, L.K., Lee, W.J., Huang, J.K., Chen, L.K., Lin, C.P., 2015. Age-related changes in resting-state networks of a large sample size of healthy elderly. CNS Neurosci. Ther. 21, 817–825.

Jack Jr., C.R., Knopman, D.S., Jagust, W.J., Shaw, L.M., Aisen, P.S., Weiner, M.W., Petersen, R.C., Trojanowski, J.Q., 2010. Hypothetical model of dynamic biomarkers of the Alzheimer's pathological cascade. Lancet Neurol. 9, 119–128.
Jenkinson, M., Beckmann, C.F., Behrens, T.E., Woolrich, M.W., Smith, S.M., 2012. FSL. NeuroImage 62, 782–790.
Johnson, S.C., Saykin, A.J., Baxter, L.C., Flashman, L.A., Santulli, R.B., Mcallister, T.W., Mamourian, A.C., 2000. The relationship between fMRI activation and cerebral atrophy: comparison of normal aging and alzheimer disease. NeuroImage 11, 179–187.
Joo, S.H., Lim, H.K., Lee, C.U., 2016. Three large-scale functional brain networks from resting-state functional MRI in subjects with different levels of cognitive impairment. Psychiatr. Investig. 13, 1–7.
Kalpouzos, G., Persson, J., Nyberg, L., 2012. Local brain atrophy accounts for functional activity differences in normal aging. Neurobiol. Aging 33, 623 e621-623 e613.
Kruskal, W.H., Wallis, W.A., 1952. Use of ranks in one-criterion variance analysis. J. Am. Stat. Assoc. 47, 583–621.
Landis, J.R., Koch, G.G., 1977. The measurement of observer agreement for categorical data. Biometrics 33, 159–174.
Lim, H.K., Nebes, R., Snitz, B., Cohen, A., Mathis, C., Price, J., Weissfeld, L., Klunk, W., Aizenstein, H.J., 2014. Regional amyloid burden and intrinsic connectivity networks in cognitively normal elderly subjects. Brain 137, 3327–3338.
Marchitelli, R., Minati, L., Marizzoni, M., Bosch, B., Bartres-Faz, D., Muller, B.W., Wiltfang, J., Fiedler, U., Roccatagliata, L., Picco, A., Nobili, F., Blin, O., Bombois, S., Lopes, R., Bordet, R., Sein, J., Ranjeva, J.P., Didic, M., Gros-Dagnac, H., Payoux, P., Zoccatelli, G., Alessandrini, F., Beltramello, A., Bargallo, N., Ferretti, A., Caulo, M., Aiello, M., Cavaliere, C., Soricelli, A., Parnetti, L., Tarducci, R., Floridi, P., Tsolaki, M., Constantinidis, M., Drevelegas, A., Rossini, P.M., Marra, C., Schonknecht, P., Hensch, T., Hoffmann, K.T., Kuijer, J.P., Visser, P.J., Barkhof, F., Frisoni, G.B., Jovicich, J., 2016. Test-retest reliability of the default mode network in a multi-centric fMRI study of healthy elderly: effects of data-driven physiological noise correction techniques. Hum. Brain Mapp. 37, 2114–2132.
Meindl, T., Teipel, S., Elmouden, R., Mueller, S., Koch, W., Dietrich, O., Coates, U., Reiser, M., Glaser, C., 2010. Test-retest reproducibility of the default-mode network in healthy individuals. Hum. Brain Mapp. 31, 237–246.
Menon, V., Uddin, L.Q., 2010. Saliency, switching, attention and control: a network model of insula function. Brain Struct. Funct. 214, 655–667.
Mitchell, A.J., Shiri-Feshki, M., 2009. Rate of progression of mild cognitive impairment to dementia–meta-analysis of 41 robust inception cohort studies. Acta Psychiatr. Scand. 119, 252–265.
Muller, R., Buttner, P., 1994. A critical discussion of intraclass correlation coefficients. Stat. Med. 13, 2465–2476.
Oldfield, R.C., 1971. The assessment and analysis of handedness: the Edinburgh inventory. Neuropsychologia 9, 97–113.
Onoda, K., Ishihara, M., Yamaguchi, S., 2012. Decreased functional connectivity by aging is associated with cognitive decline. J. Cogn. Neurosci. 24, 2186–2198.
Petersen, R.C., Smith, G.E., Waring, S.C., Ivnik, R.J., Tangalos, E.G., Kokmen, E., 1999. Mild cognitive impairment: clinical characterization and outcome. Arch. Neurol. 56, 303–308.
Petersen, R.C., Doody, R., Kurz, A., Mohs, R.C., Morris, J.C., Rabins, P.V., Ritchie, K., Rossor, M., Thal, L., Winblad, B., 2001. Current concepts in mild cognitive impairment. Arch. Neurol. 58, 1985–1992.
Power, J.D., Barnes, K.A., Snyder, A.Z., Schlaggar, B.L., Petersen, S.E., 2012. Spurious but systematic correlations in functional connectivity MRI networks arise from subject motion. NeuroImage 59, 2142–2154.
Power, J.D., Schlaggar, B.L., Petersen, S.E., 2015. Recent progress and outstanding issues in motion correction in resting state fMRI. NeuroImage 105, 536–551.
Raichle, M.E., 2011. The restless brain. Brain Connect. 1, 3–12.
Salomone, S., Caraci, F., Leggio, G.M., Fedotova, J., Drago, F., 2012. New pharmacological strategies for treatment of Alzheimer's disease: focus on disease modifying drugs. Br. J. Clin. Pharmacol. 73, 504–517.
Seeley, W.W., Menon, V., Schatzberg, A.F., Keller, J., Glover, G.H., Kenna, H., Reiss, A.L., Greicius, M.D., 2007. Dissociable intrinsic connectivity networks for salience processing and executive control. J. Neurosci. 27, 2349–2356.
Serra, L., Cercignani, M., Mastropasqua, C., Torso, M., Spano, B., Makovac, E., Viola, V., Giulietti, G., Marra, C., Caltagirone, C., Bozzali, M., 2016. Longitudinal changes in functional brain connectivity predicts conversion to Alzheimer's disease. J. Alzheimers Dis. 51, 377–389.
Shehzad, Z., Kelly, A.M., Reiss, P.T., Gee, D.G., Gotimer, K., Uddin, L.Q., Lee, S.H., Margulies, D.S., Roy, A.K., Biswal, B.B., Petkova, E., Castellanos, F.X., Milham, M.P., 2009. The resting brain: unconstrained yet reliable. Cereb. Cortex 19, 2209–2229.
Shrout, P.E., Fleiss, J.L., 1979. Intraclass correlations: uses in assessing rater reliability. Psychol. Bull. 86, 420–428.
Smyser, C.D., Inder, T.E., Shimony, J.S., Hill, J.E., Degnan, A.J., Snyder, A.Z., Neil, J.J., 2010. Longitudinal analysis of neural network development in preterm infants. Cereb. Cortex 20, 2852–2862.
Sorg, C., Riedl, V., Muhlau, M., Calhoun, V.D., Eichele, T., Laer, L., Drzezga, A., Forstl, H., Kurz, A., Zimmer, C., Wohlschlager, A.M., 2007. Selective changes of resting-state networks in individuals at risk for Alzheimer's disease. Proc. Natl. Acad. Sci. U. S. A. 104, 18760–18765.
Sperling, R., 2011. Potential of functional MRI as a biomarker in early Alzheimer's disease. Neurobiol. Aging 32 (Suppl. 1), S37–S43.
Tombaugh, T.N., 2004. Trail Making Test A and B: normative data stratified by age and education. Arch. Clin. Neuropsychol. 19, 203–214.
Van Dijk, K.R., Sabuncu, M.R., Buckner, R.L., 2012. The influence of head motion on intrinsic functional connectivity MRI. NeuroImage 59, 431–438.
Vellas, B., Aisen, P.S., Sampaio, C., Carrillo, M., Scheltens, P., Scherrer, B., Frisoni, G.B., Weiner, M., Schneider, L., Gauthier, S., Gispen-de Wied, C.C., Hendrix, S., Feldman, H., Cedarbaum, J., Petersen, R., Siemers, E., Andrieu, S., Prvulovic, D., Touchon, J., Hampel, H., 2011. Prevention trials in Alzheimer's disease: an EU-US task force report. Prog. Neurobiol. 95, 594–600.
Weiskopf, N., Hutton, C., Josephs, O., Deichmann, R., 2006. Optimal EPI parameters for reduction of susceptibility-induced BOLD sensitivity losses: a whole-brain analysis at 3 T and 1.5 T. NeuroImage 33, 493–504.
Worsley, K.J., Friston, K.J., 1995. Analysis of fMRI time-series revisited–again. NeuroImage 2, 173–181.
Wu, C.W., Chen, C.L., Liu, P.Y., Chao, Y.P., Biswal, B.B., Lin, C.P., 2011. Empirical evaluations of slice-timing, smoothing, and normalization effects in seed-based, resting-state functional magnetic resonance imaging analyses. Brain Connect. 1, 401–410.
Yan, C.G., Wang, X.D., Zuo, X.N., Zang, Y.F., 2016. DPABI: Data Processing & Analysis for (Resting-State) Brain Imaging. Neuroinformatics 14 (3), 339–351.
Yeo, B.T., Krienen, F.M., Sepulcre, J., Sabuncu, M.R., Lashkari, D., Hollinshead, M., Roffman, J.L., Smoller, J.W., Zollei, L., Polimeni, J.R., Fischl, B., Liu, H., Buckner, R.L., 2011. The organization of the human cerebral cortex estimated by intrinsic functional connectivity. J. Neurophysiol. 106, 1125–1165.
Zhang, H.Y., Wang, S.J., Liu, B., Ma, Z.L., Yang, M., Zhang, Z.J., Teng, G.J., 2010. Resting brain connectivity: changes during the progress of Alzheimer disease. Radiology 256, 598–606.
Zuo, X.N., Kelly, C., Adelstein, J.S., Klein, D.F., Castellanos, F.X., Milham, M.P., 2010. Reliable intrinsic connectivity networks: test-retest evaluation using ICA and dual regression approach. NeuroImage 49, 2163–2177.